Time evolution of the dielectric function in a three-level system under pulsed excitation

J. Y. Bigot, J. Miletic,* and B. Hönerlage
Laboratoire de Spectroscopie et d'Optique du Corps Solide, Université Louis Pasteur, 5 rue de l'Université 67000 Strasbourg, France
(Received 3 June 1985)

We calculate the dielectric function of three-level systems like CuCl under high pulsed excitation in the nanosecond time scale. We find a memory effect of the crystal absorption and dispersion which is mainly due to the radiative lifetimes of the biexcitons created during the pulse.

I. INTRODUCTION

The interaction between light and matter varies strongly with excitation intensity when photon energy of the exciting laser is close to electronic resonances. These nonlinearities give rise to anomalies in the dispersion and absorption of the samples and may, e.g., be used to obtain information about optical bistability.[1–4] In this context, semiconductors are of special interest since they are transparent below the exciton absorption line. In addition, their density is so high that the anomalies mentioned above may be studied with samples having a thickness of about 1 μm or even less. Then, the time a light pulse takes to pass through the sample is in the picosecond time scale. We are especially interested in systems like CuCl, where it was argued that a dispersive nonlinearity related to virtual biexciton formation could give rise to optical bistability.[5] If the sample is inside a Fabry-Pérot resonator, such a system may switch between two stable states on a time scale determined by the time required to change the intensity in the sample.[6–8] This time is related to the round-trip time and the reflection coefficient but does not depend on the lifetime of the elementary excitations (excitons and biexcitons) and therefore on the energy dissipation inside the sample.

Experimentally, dispersive optical bistability has been observed in CuCl,[9,10] and the switching times have been measured to be 260 and 450 ps for the off-to-on and on-to-off switchings, respectively.[11] Depending on the sample, however, switching times could be longer[12] or even hindered due to strong nonlinear absorption, which implied that the Fabry-Pérot resonator could no longer provide sufficient feedback.[13] In this context, we have observed[11] that the nonlinear transmission of CuCl without a Fabry-Pérot cavity shows hysteresis of the absorptive or dispersive type if the sample is excited by dye-laser pulses having about 8 ns duration [full width at half maximum (FWHM)]. Since the hysteresis observed in this case is of transient nature, we study the time evolution of the dielectric function in three-level systems under pulsed excitation. It is the aim of this publication to get information on the influence of the exciton and the biexciton dynamics and to discuss whether switching may happen with or without energy dissipation in these systems.

II. MODEL CALCULATION OF THE TRANSIENT DIELECTRIC FUNCTION

In the nonstationary regime, the polarization induced by a light field can be determined in the density matrix formalism from the self-consistent solution of the Maxwell and Bloch equations.[8,14–16] Since the numerical solution of the full system is quite complicated, a mean-field treatment of the Maxwell equations was adopted,[6] neglecting the exciton and biexciton dynamics.

We will follow in this work a different approach in which the population dynamics is included and only spatial propagation effects are neglected, assuming a homogeneous mean field inside the sample. We will extend here an approach discussed for the stationary regime in Refs. 17 and 18.

Let us consider a three-level system, corresponding to the crystal ground state (index 1), the exciton state $|2\rangle$, and the biexciton state $|3\rangle$, having energies 0, E_{ex}, and E_{bi}, respectively. All these states are assumed to have no spatial dispersion. This assumption is made in order to simplify the calculation of the dielectric function. In the presence of spatial dispersion, a self-consistent calculation would be required which does not lead to a better qualitative understanding of transient effects. This is also the case of inter- and intraband scattering processes which would lead to energy- and wave-vector-dependent damping functions. In addition, the quantum-statistical nature of the quasiparticles is neglected. This becomes important only at very high excitation intensities which we do not treat in this publication. At such high intensities the fermion character of the electronic excitations (excitons, biexcitons) leads to a formulation in terms of an interacting boson system, obeying neither pure boson nor fermion statistics.

A light field $A(t)$ induces transitions between the states $|1\rangle$ and $|2\rangle$ or $|2\rangle$ and $|3\rangle$, the transition between $|1\rangle$ and $|3\rangle$ being forbidden for one-photon processes. The Hamiltonian H then reads in the dipole approximation:

$$H = H_0 - \mu A(t) \ . \tag{1}$$

H_0 is the Hamiltonian of the noninteracting system and μ is the dipole operator. $A(t)$ is the time-dependent electric field for which we assume the following form:

$$A(t) = \tilde{A}(t)\cos(\omega t) \ , \tag{2}$$

where the envelope function $\tilde{A}(t)$ of the pulse is slowly varying when compared to $\cos(\omega t)$.

The polarization $P(t)$ may be expressed in terms of the density matrix $\rho(t)$ by[14,18]

$$P(t) = N\mathrm{tr}[\rho(t)\mu] \ , \tag{3}$$

where N is the density of molecules in the crystal. The matrix representation of the dipole operator μ is

$$\mu=\begin{bmatrix} 0 & \mu_{ex} & 0 \\ \mu_{ex} & 0 & \mu_{bi} \\ 0 & \mu_{bi} & 0 \end{bmatrix} . \tag{4}$$

The elements μ_{ex} and μ_{bi} are given by

$$\mu_{ex}=\langle 2 \mid \mu \mid 1 \rangle$$

and (5)

$$\mu_{bi}=\langle 3 \mid \mu \mid 2 \rangle .$$

We find from Eqs. (3)—(5)

$$P(t)=N\{[\rho_{12}(t)+\rho_{21}(t)]\mu_{ex}+[\rho_{23}(t)+\rho_{32}(t)]\mu_{bi}\} . \tag{6}$$

The time dependence of the elements of the density matrix follows from the Schrödinger equation to[14]

$$\frac{\partial\rho_{ij}(t)}{\partial t}=\frac{i}{\hbar}[\rho(t),H]_{ij}-\rho_{ij}(t)\Gamma_{ij} \tag{7}$$

$[i,j\in(1,2,3)]$, where the damping constants Γ_{ij} account for coherence relaxation ($j\neq i$) and for population lifetimes ($i=j$).

Equation (7) gives rise to a set of coupled differential equations. We obtain for the off-diagonal elements

$$\begin{aligned}
\frac{\partial\rho_{12}}{\partial t}&=\frac{i}{\hbar}[-\mu_{ex}A(t)(\rho_{11}-\rho_{22})+\rho_{12}E_{ex} \\
&\quad -\rho_{13}\mu_{bi}A(t)]-\Gamma_{12}\rho_{12} , \\
\frac{\partial\rho_{13}}{\partial t}&=\frac{i}{\hbar}[A(t)(\mu_{ex}\rho_{23}-\mu_{bi}\rho_{12})+\rho_{13}E_{bi}]-\Gamma_{13}\rho_{13} , \\
\frac{\partial\rho_{23}}{\partial t}&=\frac{i}{\hbar}[-\mu_{bi}A(t)(\rho_{22}-\rho_{33})+\rho_{23}(E_{bi}-E_{ex}) \\
&\quad +\mu_{ex}A(t)\rho_{13}]-\Gamma_{23}\rho_{23} .
\end{aligned} \tag{8}$$

The difference of population between two states i and j and their corresponding time evolution are derived from equation (7) to

$$\begin{aligned}
\frac{\partial(\rho_{11}-\rho_{22})}{\partial t}&=-\frac{i}{\hbar}A(t)[2\mu_{ex}(\rho_{12}-\rho_{21})-\mu_{bi}(\rho_{23}-\rho_{32})] \\
&\quad -[(\rho_{11}-\rho_{22})-(\rho_{11}-\rho_{22})_0]\Gamma_1 , \\
\frac{\partial(\rho_{22}-\rho_{33})}{\partial t}&=\frac{i}{\hbar}A(t)[\mu_{ex}(\rho_{12}-\rho_{21})-2\mu_{bi}(\rho_{23}-\rho_{32})] \\
&\quad -[(\rho_{22}-\rho_{33})-(\rho_{22}-\rho_{33})_0]\Gamma_1' ,
\end{aligned} \tag{9}$$

where $(\rho_{ii}-\rho_{jj})_0$ give the equilibrium distribution of the population difference between the states $|i\rangle$ and $|j\rangle$ in the absence of the external field $A(t)$, $(\rho_{ii}-\rho_{jj})$ their actual time-dependent values, and $1/\Gamma_1$ and $1/\Gamma_1'$ are their respective lifetimes.

We now develop the density matrix elements $\rho_{ij}(t)$ into a series in order to separate fast and slowly varying contributions:[19]

$$\rho_{ij}(t)=\sum_n \rho_{ij}^n(t)e^{in\omega t} . \tag{10}$$

Equation (10) becomes a Fourier series in the stationary regime, i.e., if the ρ_{ij}^n are independent of time. Inserting Eq. (10) into Eq. (6), we obtain

$$\begin{aligned}
P(t)=N\sum_n \{&[\rho_{12}^n(t)+\rho_{21}^n(t)]\mu_{ex} \\
&+[\rho_{23}^n(t)+\rho_{32}^n(t)]\mu_{bi}\}e^{i\omega t} .
\end{aligned} \tag{11}$$

On the other hand, $P(t)$ is given in the nonstationary regime in terms of susceptibility (neglecting spatial dispersion),

$$P(t)=\epsilon_0 \mathrm{Re}\left[\int_{-\infty}^{t}\chi(t,t')A'(t')dt'\right] , \tag{12}$$

where $A'(t')$ is the complex electric field of the form

$$A'(t')=\tilde{A}'(t')e^{i\omega t'} . \tag{13}$$

If $\tilde{A}'(t')$ were constant, $\chi(t,t')$ would depend only on the time difference $t-t'=\tau$. Introducing $t'=t-\tau$ in Eq. (13), we obtain

$$P(t)=\epsilon_0 \mathrm{Re}\left[\int_0^{\infty}\chi(t,\tau)\tilde{A}'(t-\tau)e^{i\omega(t-\tau)}d\tau\right] . \tag{14}$$

If the field amplitude is "slowly" varying during the response time of the system [i.e., $\chi(t,\tau)$ is large during this time interval and small outside], we may approximate

$$\begin{aligned}
P(t)&\approx\epsilon_0 \mathrm{Re}\left[\tilde{A}'(t)e^{i\omega t}\int_0^{\infty}\chi(t,\tau)e^{-i\omega\tau}d\tau\right] \\
&=\epsilon_0 \mathrm{Re}\left[\tilde{A}'(t)\chi(t,\omega)e^{i\omega t}\right] .
\end{aligned} \tag{15}$$

This may be rewritten[14] as

$$P(t)=\epsilon_0\tilde{A}(t)[\chi'(t,\omega)\cos(\omega t)-\chi''(t,\omega)\sin(\omega t)] , \tag{16}$$

where $\chi'=\mathrm{Re}\chi$ and $\chi''=\mathrm{Im}\chi$.

When comparing with Eq. (11), we find the time-dependent susceptibility at frequency ω in the above approximation:

$$\begin{aligned}
\chi(t,\omega)=\frac{2N}{\epsilon_0\tilde{A}(t)}\{&[\rho_{12}^1(t)+\rho_{21}^1(t)]\mu_{ex} \\
&+[\rho_{23}^1(t)+\rho_{32}^1(t)]\mu_{bi}\} .
\end{aligned} \tag{17}$$

Since $\chi(t,\omega)$ is expressed by the nondiagonal elements $\rho_{ij}^1(t)$, the important time constants relevant in our slowly varying envelope approximation are the dephasing times $1/\Gamma_{12}$ and $1/\Gamma_{23}$, which are in the picosecond time scale in CuCl.[20,21] They determine the time interval considered in the approximation of Eq. (15). Inserting Eq. (10) into (8) and (9), we obtain a set of recurrence relations involving the different functions $\rho_{ij}^n(t)$:

$$i\hbar\frac{\partial\rho_{12}^n(t)}{\partial t}=-(E_{ex}-n\hbar\omega+i\hbar\Gamma_{12})\rho_{12}^n(t)+\frac{\mu_{bi}\tilde{A}(t)}{2}[\rho_{13}^{n-1}(t)+\rho_{13}^{n+1}(t)]+\frac{\mu_{ex}\tilde{A}(t)}{2}[(\rho_{11}-\rho_{22})^{n-1}(t)+(\rho_{11}-\rho_{22})^{n+1}(t)]\ ,$$

$$i\hbar\frac{\partial\rho_{13}^n(t)}{\partial t}=-(E_{bi}-n\hbar\omega+i\hbar\Gamma_{13})\rho_{13}^n(t)+\mu_{bi}\tilde{A}(t)[\rho_{12}^{n-1}(t)+\rho_{12}^{n+1}(t)]-\frac{\mu_{ex}\tilde{A}(t)}{2}[\rho_{23}^{n-1}(t)+\rho_{23}^{n+1}(t)]\ ,$$

$$i\hbar\frac{\partial\rho_{23}^n(t)}{\partial t}=-(E_{bi}-E_{ex}-n\hbar\omega+i\hbar\Gamma_{23})\rho_{23}^n(t)-\frac{\mu_{ex}\tilde{A}(t)}{2}[\rho_{13}^{n-1}(t)+\rho_{13}^{n+1}(t)]$$
$$+\frac{\mu_{bi}\tilde{A}(t)}{2}[(\rho_{22}-\rho_{33})^{n-1}(t)+(\rho_{22}-\rho_{33})^{n+1}(t)]\ , \tag{18}$$

$$-i\hbar\frac{\partial}{\partial t}(\rho_{11}-\rho_{22})^n(t)=-i\hbar\Gamma_1\delta_{n,0}-(n\hbar\omega-i\hbar\Gamma_1)(\rho_{11}-\rho_{22})^n(t)+\frac{\mu_{bi}\tilde{A}(t)}{2}[\rho_{23}^{n-1}(t)-\rho_{32}^{n-1}(t)+\rho_{23}^{n+1}(t)-\rho_{32}^{n+1}(t)]$$
$$-\mu_{ex}\tilde{A}(t)[\rho_{12}^{n-1}(t)-\rho_{21}^{n-1}(t)+\rho_{12}^{n+1}(t)-\rho_{21}^{n+1}(t)]\ ,$$

$$-i\hbar\frac{\partial}{\partial t}(\rho_{22}-\rho_{33})^n(t)=-(n\hbar\omega-i\hbar\Gamma_1')(\rho_{22}-\rho_{33})^n+\frac{\mu_{ex}\tilde{A}(t)}{2}[\rho_{12}^{n-1}(t)-\rho_{21}^{n-1}(t)+\rho_{12}^{n+1}(t)-\rho_{21}^{n+1}(t)]$$
$$-\mu_{bi}\tilde{A}(t)[\rho_{23}^{n-1}(t)-\rho_{32}^{n-1}(t)+\rho_{23}^{n+1}(t)-\rho_{32}^{n+1}(t)]\ .$$

In Eq. (18), we have assumed that the system is in its ground state before it is excited by the external field $A(t)$. We thus obtain an infinite set of coupled linear differential equations which we restrict to the functions $(\rho_{11}-\rho_{22})^0(t)$, $(\rho_{22}-\rho_{33})^0(t)$, $\rho_{12}^1(t)$, $\rho_{21}^1(t)$, $\rho_{13}^2(t)$, $\rho_{31}^2(t)$, $\rho_{23}^1(t)$, $\rho_{32}^1(t)$, and their complex-conjugate expressions. In Ref. 18, we have included all the terms ρ_{ij}^n and we could show that the choice given above describes the dielectric function in the steady-state regime within a very good approximation. The system of coupled equations is now solved numerically, and Eq. (17) gives the dielectric susceptibility $\chi(t)$. It is applied to CuCl, where the relevant exciton and biexciton parameters are well known[20–24] for small values of excitation energy . As discussed in more detail in Refs. 17 and 18, the dipole matrix elements μ_{ex} and μ_{bi} are given by

$$N\mu_{ex}^2=\epsilon_0\epsilon_b(E_L^2-E_{ex}^2)/2/E_{ex}$$

and (19)

$$\mu_{bi}^2\tilde{A}^2(t)=4M^2n_p(t)\ ,$$

respectively. $\epsilon_b=5$ is the background dielectric constant, $E_L=3.208$ eV and $E_{ex}=3.2025$ eV are the energies of the longitudinal and transverse exciton.[23] $M^2=2.1\times10^{-22}$ eV^2 cm^3 is the exciton-biexciton transition matrix element[20] and $n_p(t)$ the density of polaritons in the sample. The biexciton energy $E_{bi}=6.372$ eV is well known from two-photon absorption studies[20] and the relaxation times are assumed to be such that $\hbar\Gamma_1=10^{-6}$ eV and $\hbar\Gamma_{12}=\hbar\Gamma_{23}=10^{-4}$ eV.[20–22] Concerning the pulse envelope $|\tilde{A}(t)|^2$, we assume a Gaussian pulse of 600 ps half-width and a maximum photon density of $n_p=4\times10^{15}$ cm^{-3} superimposed on a constant amplitude of $n_p=10^6$ cm^{-3} because of numerical reasons. As shown in Fig. 1, $|\tilde{A}(t)|$ is maximum at a time $t=800$ ps.

Using these parameters, we may now calculate the dielectric function given by

$$\epsilon/\epsilon_0=\epsilon_b+\chi\ .$$

Now, we define as in the stationary case the polariton wave vector Q, the absorption coefficient α, and the reflection coefficient R by the relations

$$Q=\frac{\omega}{\sqrt{2}c}\{\mathrm{Re}\epsilon+[(\mathrm{Re}\epsilon)^2+(\mathrm{Im}\epsilon)^2]^{1/2}\}^{1/2}\ ,$$
$$\alpha=\frac{\omega}{\sqrt{2}c}\{-\mathrm{Re}\epsilon+[(\mathrm{Re}\epsilon)^2+(\mathrm{Im}\epsilon)^2]^{1/2}\}^{1/2}\ . \tag{20}$$

Q and α are related to the real (n') and imaginary (n'') part of the refractive index by

$$n'=\frac{Qc}{\omega}$$

and (21)

$$n''=\frac{c\alpha}{\omega}\ ,$$

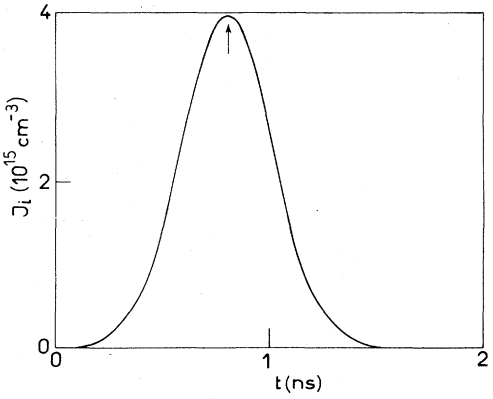

FIG. 1. Time dependence of the incident pulse.

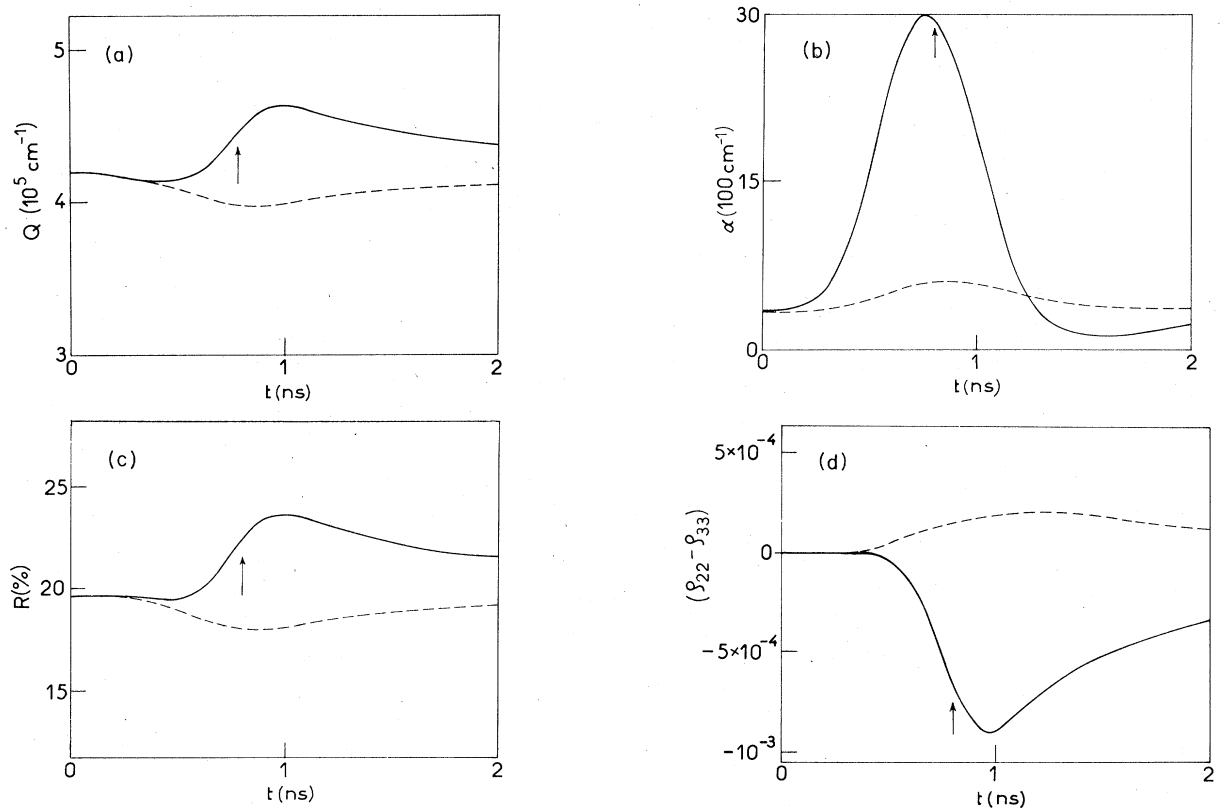

FIG. 2. (a) Wave vector Q; (b) absorption coefficient α; (c) reflection coefficient R; and (d) population inversion $\rho_{22}-\rho_{33}$ as functions of time under pulsed excitation, using $\hbar\omega=3.1865$ eV and $\hbar\Gamma_{13}=4\times10^{-4}$ eV. V (solid line) and $\hbar\Gamma_{13}=2.5\times10^{-5}$ eV (dashed line). The maximum of the incident pulse is indicated by the arrow.

and the reflection coefficient R is defined by

$$R=[(n'-1)^2+n''^2]/[(n'+1)^2+n''^2]\ . \tag{22}$$

III. NUMERICAL RESULTS AND DISCUSSION

Figure 2 gives the variation of Q, α, and R, defined in Eqs. (20) to (22) as functions of time during the pulse given in Fig. 1. The arrow indicates in all figures the maximum of the pulse intensity. The energy of the exciting photons is at 3.1865 eV (i.e., above half the biexciton energy). One should be reminded here that the order of magnitude of the different damping constants is known at low intensities of excitation; a detailed analysis shows, however, that the dampings depend on the intensity of excitation and on the photon energy. Since we are mainly interested in the spectral region around half the biexciton energy, we have varied Γ_{13} and Γ_1'. The other damping parameters were found to be of minor influence. Concerning the solid lines in Fig. 2, the damping constants $\hbar\Gamma_{13}=4\times10^{-4}$ eV and $\hbar\Gamma_1'=5\times10^{-7}$ eV are chosen. We clearly see that the plots of all physical quantities are asymmetrical with respect to the maximum value of the exciting pulse. This asymmetry decreases if the biexciton relaxation constant Γ_1' is increased, indicating that the system returns to its equilibrium value more quickly, and the asymmetry vanishes for $\hbar\Gamma_1'>10^{-4}$ eV. The exciton relaxation constant Γ_1, however, has no influence on the asymmetry when it is increased up to a value of $\hbar\Gamma_1=10^{-3}$ eV. The damping constants Γ_{12} and Γ_{23} have minor influence on the asymmetry near the biexciton resonance. In order to discuss the physical origin of the asymmetry of Q, α, and R, we give in Fig. 2(d), the time dependence of the exciton-biexciton population difference $(\rho_{22}-\rho_{33})(t)$. If this quantity is constant or follows the pulse shape instantaneously, Q or α (and therefore R) also

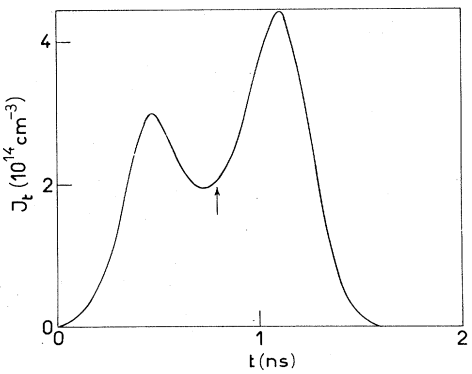

FIG. 3. Transmitted pulse when calculated from Figs. 1 and 2. The maximum of the incident pulse is indicated by the arrow.

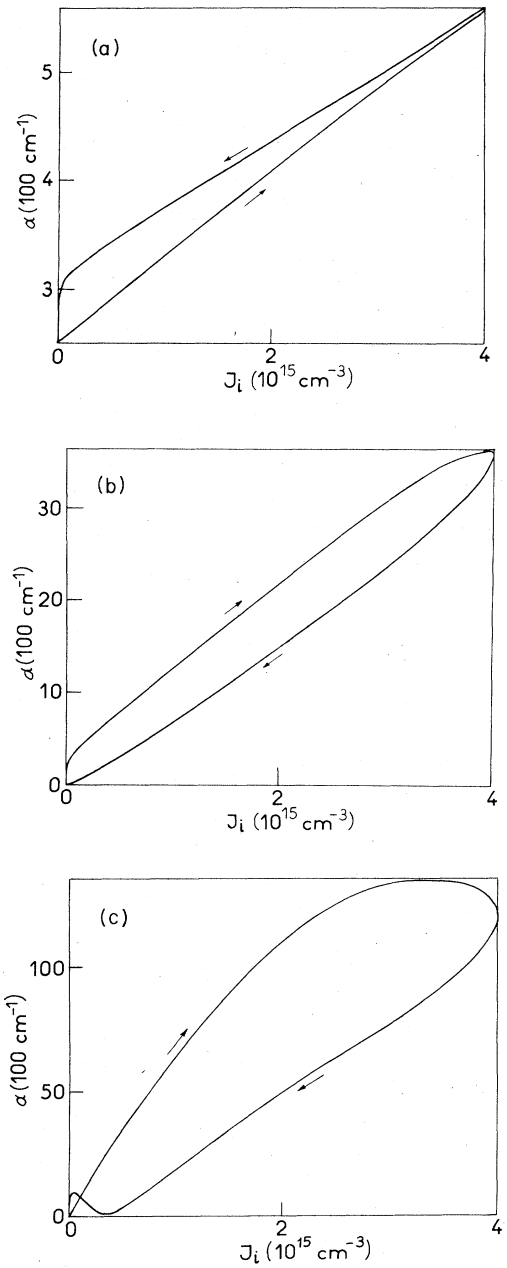

FIG. 4. Absorption coefficient α as function of the excitation intensity during the pulse, with $\hbar\Gamma_{13}=4\times10^{-4}$ eV and for different energies of excitation near half the biexciton energy. The arrows denote the sense of the hysteresis for increasing and decreasing intensity of excitation: (a) $\hbar\omega=3.184$ eV; (b) $\hbar\omega=3.1855$ eV; (c) $\hbar\omega=3.186$ eV. Above half the biexciton energy, for $\hbar\omega=3.1865$ and 3.188 eV, the hysteresis loops are similar to those at $\hbar\omega=3.1855$ and 3.184 eV, respectively.

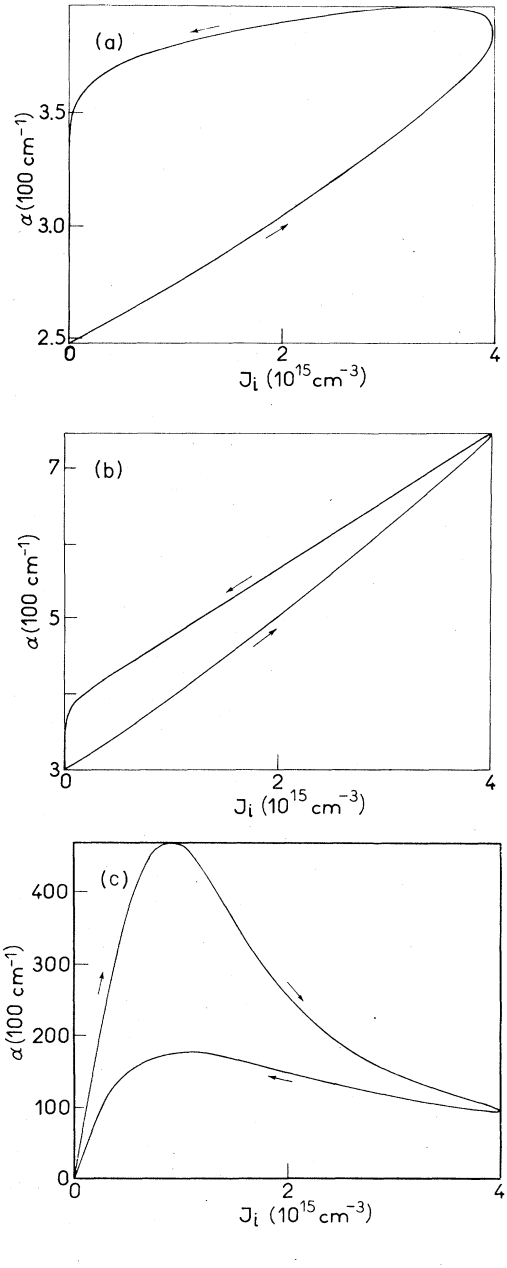

FIG. 5. The same parameters as in Fig. 4, but with $\hbar\Gamma_{13}=2.5\times10^{-5}$ eV.

follow the shape of the pulse.

Although the constant $1/\Gamma_{13}$ (defining the biexciton dephasing time) is small with respect to the envelope variation during the pulse, it has nevertheless an important influence on the variation of Q, α, and R. This is indicated in Fig. 2 by choosing $\hbar\Gamma_{13}=2.5\times10^{-5}$ eV (dashed lines). Q and R diminish during the pulse with increasing intensity while for $\hbar\Gamma_{13}=4\times10^{-4}$ eV they increase (solid line). The absorption α reaches a higher value than the equilibrium value (330 cm^{-1}) at the end of the pulse, while in the first case (solid line) it is below this value. Comparing dashed and dotted lines in Figs. 2(b) and 2(d), we note that, for smaller values of Γ_{13}, the nonlinear absorption is much smaller, which is due to the fact that the population difference $(\rho_{22}-\rho_{33})$ is positive (dashed line) while we obtain an inversion of the population $[(\rho_{22}-\rho_{33})<0]$ for $\Gamma_{13}=4\times10^{-4}$ eV (solid line). This can be explained by the fact that if Γ_{13} is large, biexcitons are more easily created if the exciting source is detuned from the biexci-

ton resonance, since Γ_{13} increases the biexciton linewidth. The biexciton density becomes higher than that of excitons and their dynamics then governs the "memory effect" of Q, α, and R. As shown in Fig. 3, this memory effect may lead to an asymmetric pulse deformation.[11] In this case, we have calculated the transmitted intensity $I_t(t)$ of the pulse of Fig. 1 with the incident intensity $I_i(t)$, assuming a crystal of thickness $l=5$ μm and showing the uniform absorption $\alpha(t)$ given in Fig. 2(b) (solid line):

$$I_t(t)=I_i(t)e^{-\alpha(t)l}[1-R(t)]^2 . \tag{23}$$

If transmission experiments are analyzed and $\alpha(I_i(t))$ is plotted,[11] the absorption shows hysteresis. As shown in Fig. 4, for $\Gamma_{13}=4\times10^{-4}$ eV, the direction of this hysteresis loop changes with the energy of excitation near half the biexciton energy due to the inversion of population $\rho_{22}-\rho_{33}$ which may occur.

As shown in Fig. 5, the hysteresis loops change their form qualitatively if $\Gamma_{13}=2.5\times10^{-5}$ eV is chosen, since the resonance character of the biexciton creation is more pronounced. We will not try to give here a quantitative agreement with the results of Ref. 11, since our mean-field approximation will break down at very high absorption values [Figs. 4(c) and 5(c)] and propagation effects come into play. In addition, our model calculation assumes constant values for the damping; in real systems however they also depend on the population density.[25–29] Their variation during the pulse may also give rise to hysteresis or even bistability as it was reported for two-level systems.[30–32] In addition, the qualitative features of Q, α, and $\rho_{22}-\rho_{33}$ remain the same for different pulse shapes, while their quantitative dependence is different.

IV. CONCLUSION

We have discussed the time evolution of the dielectric function in CuCl. The population of biexcitons gives rise to a memory effect, which has been observed recently. The fast dephasing time Γ_{13} has an influence on the nonlinear absorption and thus changes the population inversion $(\rho_{22}-\rho_{33})$ between excitons and biexcitons during the pulse. Their dynamics, however, is governed by their lifetime and for high damping constants they follow the envelope of the exciting pulse, i.e., the stationary regime.

ACKNOWLEDGMENTS

The authors are grateful to Professor H. Haug for his interest in their work and to Drs. J. B. Grun, R. Levy, F. Tomasini, and M. Frindi for many stimulating discussions and careful reading of the manuscript. This work was supported by a contract from the Ministère des Postes, Téléphones et Télécommunications of France-Direction Générale des Télécommunications-Direction des Affaires Industrielles et Internationales. It has been carried out in the framework of an operation launched by the Commission of the European Communities under the experimental phase of the European Community Stimulation Action. The Laboratoire de Spectroscopie et d'Optique du Corps Solide is "Unité Associeé au Centre National de la Recherche Scientique No. 232."

*Permanent address: Université du Québec à Trois-Rivières C.P. 500, Trois Rivières, Québec, Canada.

[1]*Optical Bistability,* edited by C. M. Bowden, M. Ciftan, and H. R. Robl (Plenum, New York 1981); *Optical Bistability II,* edited by C. M. Bowden, H. M. Gibbs, and S. L. McCall (Plenum, New York, 1984).

[2]E. Abraham and S. D. Smith, Rep. Prog. Phys. **45**, 815 (1982).

[3]L. A. Lugiato, in *Progress in Optics,* edited by E. Wolf (Elsevier, New York, 1984), Vol. XXI, pp. 69–216.

[4]H. Haug, *Festkörper Probleme,* Vol. XXII of *Advances in Solid State Physics* (Vieweg, Braunschweig, 1982), pp. 149–171.

[5]S. W. Koch and H. Haug, Phys. Rev. Lett. **46**, 450 (1981).

[6]E. Hanamura, Solid State Commun., **38**, 939 (1981).

[7]C. C. Sung and C. M. Bowden, J. Opt. Soc. Am. B **1**, 395 (1984).

[8]J. W. Haus, C. M. Bowden, and C. C. Sung, Phys. Rev. A **31**, 1936 (1985).

[9]B. Hönerlage, J. Y. Bigot, and R. Levy, in *Optical Bistability II,* Ref. 1, pp. 253–258.

[10]N. Peyghambarian, H. M. Gibbs, D. A. Weinberger, M. C. Rushford, and D. Sarid, in *Optical Bistability II,* Ref. 1, pp. 259–266.

[11]J. Y. Bigot, F. Fidorra, C. Klingshirn, and J. B. Grun, IEEE J. Quantum Electron. (to be published).

[12]R. Levy, B. Hönerlage, and J. B. Grun, Philos. Trans. R. Soc. London, Ser. A **313**, 229 (1984).

[13]J. B. Grun, B. Hönerlage, and R. Levy, J. Lumin. **30**, 217 (1985).

[14]A. Yariv, *Quantum Electronics,* 2nd ed. (Wiley, New York, 1975).

[15]S. L. McCall and E. L. Hahn, Phys. Rev. **183**, 457 (1969).

[16]J. Goll and H. Haken, Phys. Rev. A **18**, 2241 (1978).

[17]J. Y. Bigot and B. Hönerlage, Phys. Status Solidi B **121**, 649 (1984).

[18]B. Hönerlage and J. Y. Bigot, Phys. Status Solidi B **124**, 221 (1984).

[19]A. Schenzle and R. G. Brewer, Phys. Rev. A **14**, 1756 (1976).

[20]Vu Duy Phach, A. Bivas, B. Hönerlage, and J. B. Grun, Phys. Status Solidi B **84**, 731 (1977).

[21]Vu Duy Phach, A. Bivas, B. Hönerlage, and J. B. Grun, Phys. Status Solidi B **86**, 159 (1978).

[22]R. Levy, B. Hönerlage, and J. B. Grun, Phys. Rev. B **19**, 2326 (1979).

[23]B. Hönerlage, A. Bivas, and Vu Duy Phach, Phys. Rev. Lett. **41**, 49 (1978).

[24]For a review on biexcitons in CuCl, see J. B. Grun, B. Hönerlage, and R. Levy, in *Excitons,* edited by E. I. Rashba and M. D. Sturge (North-Holland, Amsterdam, 1982), Vol. 2, pp. 459–504; D. S. Chemla and A. Maruani, Prog. Quantum Electron. **8**, 1 (1982); B. Hönerlage, R. Levy, J. B. Grun, C. Klingshirn, and K. Bohnert, Phys. Rep. **124**, 161 (1985).

[25]T. Itoh, T. Katohno, and M. Ueta, J. Phys. Soc. Jpn. **53**, 844

(1984).
[26]N. Peyghambarian, L. L. Chase, and A. Mysyrowicz, Opt. Commun. **42**, 51 (1982).
[27]M. Ojima, T. Kushida, S. Shionoya, T. Tanaka, and Y. Oka, J. Phys. Soc. Jpn. **45**, 884 (1978).
[28]Y. Masumoto and S. Shionoya, Solid State Commun. **41**, 147 (1982).
[29]M. Kuwata, T. Mita, and N. Nagasawa, J. Phys. Soc. Jpn. **50**, 2467 (1981).
[30]Y. Toyozawa, Solid State Commun. **32**, 13 (1979).
[31]Hoang Xuan Nguyen and R. Zimmermann, Phys. Status Solidi B **124**, 191 (1984).
[32]S. W. Koch, H. E. Schmidt, and H. Haug, J. Lumin. **30**, 232 (1985).